Journal of Process Management and New Technologies
www.japmnt.com ISSN: 2334-735X (Print) ISSN: 2334-7449 (Online)
Vol. 10, Issue 1-2, 2022, pp. 1-16

BEAM-TYPE ACOUSTIC METAMATERIAL DESIGN FOR VIBRATION SUPPRESSION WITH STRUCTURAL DAMPING

Tianqi ZHAO[1], Tao CHEN[2]*, Wensheng MA[3]

[1]*Harbin Engineering University, College of Mathematical Sciences, Harbin 150001, PR China, 813287275@qq.com*

[2]*Harbin Engineering University, College of Mathematical Sciences, Harbin 150001, PR China, taochen@hrbeu.edu.cn*

[3]*Harbin Engineering University, College of Aerospace and Civil Engineering, Harbin 150001, PR China, 95710978@qq.com*

Abstract: *Vibration suppression of a beam-type acoustic metamaterial with periodic cavities filled by a viscoelastic membrane that supports a hollow mass still filled by a viscoelastic membrane that supports a local resonator is investigated. First, the proposed beam-type acoustic metamaterial is modeled as a one-dimensional mass-in-mass-in-mass (MMM) lumped parameter chain with structural damping, and then a mass-in-mass (MM) lumped parameter chain with structural damping is also given for comparison. For the two chains, the influence of structural damping on band structures are considered, and the loss factors associated with all propagating Bloch modes are compared. Finally, as an example, the beam-type metamaterials based on MM model with structural damping and MMM model with structural damping are designed to suppress vibration, respectively. The viscoelastic membranes act as structural damping. The finite element method based on Kirchhoff's plate theory is developed to capture dynamic displacement fields of different metamaterials. Structural frequency response is calculated for different configurations of cantilevered structures when disturbance is considered. The results show that the proposed beam-type acoustic metamaterial based on MMM model with structural damping has higher dissipation and display high damping and does not sacrifice stiffness than MM model with structural damping.*

Keywords: *Acoustic metamaterial, structural damping, band structure, elastic wave attenuation*

Original scientific paper
Received: 15.01.2022
Accepted: 08.02.2022
Available online: 14.02.2022

* Corresponding author

1. Introduction

At present, the research on the propagation characteristics of elastic waves in periodic structural materials is very popular, mainly because the propagation of elastic waves in periodic structural materials will generate band gaps (Hussein et al., 2014; Nouh et al., 2016; Galich, et al., 2017; Muhammad & Lim, 2019; An et al., 2020; Cinefra et al., 2021; Zhou et al., 2021). Elastic wave bandgap materials, also known as phononic crystals, block the propagation of elastic waves in specific frequency bands due to the periodic distribution of elastic constants and densities. This specific performance makes elastic wave bandgap materials have significant application prospects in vibration and noise reduction, guided wave, acoustic control device design and other aspects (Benchabane et al., 2006; Li et al., 2018; Suobin et al., 2019; Gao et al., 2019). Phononic crystals are based on Bragg scattering, so the lattice constant of the phononic crystals must be large enough to from a band gap.

The appearance of locally resonant phononic crystals changes the understanding that only large size structures can have low frequency band gap effect. The physical mechanism of band gap generation in locally resonant phononic crystals is different from Bragg scattering, which is determined by the resonant characteristics of local resonant units. By proper adjustment of the microstructure, the rapid attenuation of low frequency vibration energy can be realized in a small number of periodic microstructures (Zhu et al., 2011; Li et al., 2020). This periodic materials and structures are called metamaterials with local resonances, with a high level of dissipation while having high stiffness (Liu et al., 2000). The vibrational properties of acoustic metamaterials with periodic local resonances have been extensively studied. Acoustic metamaterials can be classified into intrinsic metamaterials and inertial metamaterials (Fok et al., 2008). Intrinsic acoustic metamaterials need inclusions with low phase velocity (Ding et al., 2007). Inertial acoustic metamaterials employ mass-spring-damper subsystems as local resonant and the inertial forces of the subsystems under resonance work against the excitation and attenuate the vibration (Peng et al., 2015). Hussein and Frazier (2013) derived the dispersion relation of a locally resonant metamaterial with viscous damping. Broadband vibration attenuation needs to satisfy both the two basic conditions for the presence of local resonance elements and the components capable of exhibiting damping in the metamaterial components. It is proved that a damping phenomenon called “metadamping” occurs and that damping is a necessary factor for attenuation of propagation modes outside the stop band ranges (Pai, 2010; Sun et al., 2010; Pai et al., 2014; Raghavan et al., 2013; Cenedese, 2021). Nouh et al. (2014) presented the characteristics of metamaterial beams manufactures of assemblies of periodic cells with built-in local resonances based on this kind of acoustic metamaterial design principle. Wang et al. (2016) presented a kind of metamaterial plate employing mass-spring-damper subsystems for the purpose of suppressing flexural wave propagation. Li et al. (2017) demonstrate the low frequency broadband elastic wave attenuation and vibration suppression by using plate-type elastic metamaterial employing mass-spring-damper subsystems. Zhong et al. (2021) proposed a composite under- water honeycomb-type acoustic metamaterial (rubber-steel-rubber) plate and studied the formation of its local resonance band gap (Huang et al., 2010; Chen et al., 2016). However, to our knowledge, no work

on the acoustic metamaterial design for elastic wave attenuation and vibration suppression with structural damping has been published.

This paper is aimed to design a beam-type acoustic metamaterial for elastic wave attenuation and vibration suppression with structural damping. The acoustic metamaterial is modeled as a one-dimensional MMM lumped parameter chain with structural damping, and then a typical MM lumped parameter chain with structural damping is also given for comparison. The MMM lumped parameter chain exhibits higher dissipation. So an acoustic metamaterial design principle is presented, and four kind of different beam-type acoustic metamaterials with high damping and high stiffness are designed based on this paradigm.

This organizational structure of this paper is as follows. In Section 2, the beam-type acoustic metamaterials are designed, which metamaterial has periodic cavities filled by viscoelastic membrane that supports a hollow mass still filled by a viscoelastic membrane that supports a local resonator. The metamaterial is modeled as a one-dimensional MMM lumped parameter chain with structural damping. In Section 3, an energy-based approach finite element model is presented based on Kirchhoff's plate theory, and then used to derive the governing equations of motion of the acoustic metamaterial in transverse vibration. In Section 4, numerical simulation is presented. Frequency responses of different beam prototypes are analyzed and shown. The Section 5 is the conclusion.

2. MMM model and MM model of the beam-type acoustic metamaterials

By considering lumped masses, springs, and damper elements, the designed beam-type acoustic metamaterial is modeled as a one-dimensional MMM lumped parameter chain with structural damping, and for comparison a typical MM lumped parameter chain with structural damping is also given. The motion equations and dispersion relation of the two chains are derived, and the damping ratios corresponding to all propagating Bloch modes are compared. Accordingly, the beam-type acoustic metamaterials are designed based on these results.

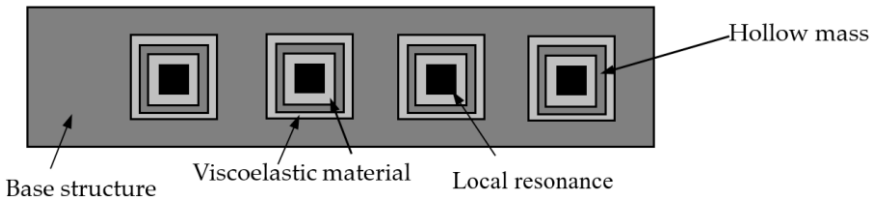

Figure 1. Schematic diagram of the beam-type acoustic metamaterial

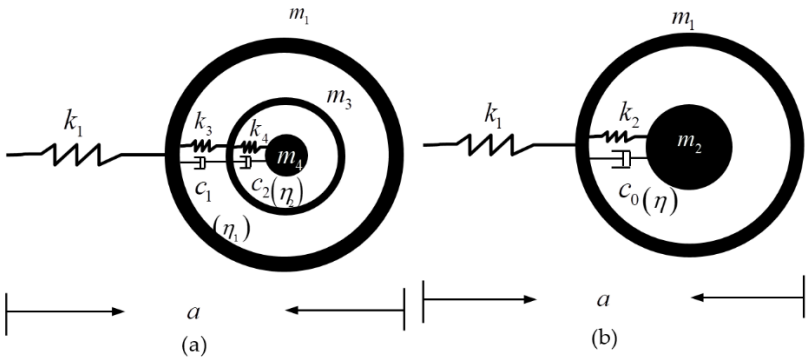

Figure 2. Unit cells of (a) MMM model and (b) MM model

The beam-type acoustic metamaterial in question has periodic cavities. The cavity is filled with a viscoelastic membrance (structural damping) to support the hollow mass. The hollow mass is still filled with a viscoelastic film (structural damping) that supports a local resonator.Fig.1 provides a schematic of a beam-type acoustic metamaterial. Fig. 2(a) and (b) are the cells of two models, respectively.

2.1. MMM model

Considering unit cell periodicity, motion equations of MMM model is obtained as follows

$$m_1\ddot{u}_1^n + k_1(2u_1^n - u_1^{n-1} - u_1^{n+1}) + k_3(u_1^n - u_3^n) + c_1(\dot{u}_1^n - \dot{u}_3^n) = 0 \ , \tag{1a}$$

$$m_3\ddot{u}_3^n + k_3(u_3^n - u_1^n) + k_4\left(u_3^n - u_4^i\right) + c_1(\dot{u}_3^n - \dot{u}_1^n) + c_2(\dot{u}_3^n - \dot{u}_4^n) = 0 \ , \tag{1b}$$

$$m_4\ddot{u}_4^n + k_4(u_4^n - u_3^n) + c_2(\dot{u}_4^n - \dot{u}_3^n) = 0 \ , \tag{1c}$$

where u_l^n is the displacement of mass l in an arbitrary nth unit cell.

By applying Bloch's theorem, we assume a plane wave solution

$$u_l^n = U_l exp(i(kx + nka) + \lambda t) = q_l(t)exp\big(i(kx + nka)\big), \tag{2}$$

whereU_l, k, x and t denote wave amplitude, wave number, position and time, respectively. Particularly, $\lambda = i\omega$ when damping is neglected.

For the case of viscous damping, dispersion relation of MMM model has been analyzed [30]. We only consider relation with structural damping here.

When structural damping is considered, dissipation force $f = c\dot{u} = i\eta ku$, where η is loss factor, k is stiffness coefficient, and u denotes displacement. Eq. (1a), (1b) and (1c) can be rewritten as

$$m_1\ddot{u}_1^n + k_1(2u_1^n - u_1^{n-1} - u_1^{n+1}) + k_3(u_1^n - u_3^n) + i\eta_1 k_3(u_1^n - u_3^n) = 0\,, \tag{3a}$$

$$m_3\ddot{u}_3^n + k_3(u_3^n - u_1^n) + k_4\left(u_3^n - u_4^i\right) + i\eta_1 k_3(u_3^n - u_1^n) + i\eta_2 k_4(u_3^n - u_4^n) = 0, \tag{3b}$$

$$m_4\ddot{u}_4^n + k_4(u_4^n - u_3^n) + i\eta_2 k_4(u_4^n - u_3^n) = 0, \tag{3c}$$

Combining Eq. (3a), (3b), (3c) and (2), we have

$$\boldsymbol{M\ddot{q}+iK_1q+Kq=0} \tag{4}$$

Where $\boldsymbol{M}=\begin{bmatrix} m_1 & 0 & 0 \\ 0 & m_3 & 0 \\ 0 & 0 & m_4 \end{bmatrix}$, $\boldsymbol{K}_1=\begin{bmatrix} \eta_1 k_3 & -\eta_1 k_3 & 0 \\ -\eta_1 k_3 & \eta_1 k_3+\eta_2 k_4 & -\eta_2 k_4 \\ 0 & -\eta_2 k_4 & \eta_2 k_4 \end{bmatrix}$,

$\boldsymbol{K}=\begin{bmatrix} 2k_1+k_3-k_1e^{ika}-k_1e^{-ika} & -k_3 & 0 \\ -k_3 & k_3+k_4 & -k_4 \\ 0 & -k_4 & k_4 \end{bmatrix}$.

Let $\eta_1/\eta_2=\bar{\eta}$, Then coefficient matrices of Eq. (4) can be rewritten

$$\boldsymbol{M}=\frac{1}{\omega_{|r|}{}^2}\begin{bmatrix} \bar{m} & 0 & 0 \\ 0 & \tilde{m} & 0 \\ 0 & 0 & 1 \end{bmatrix},\ \boldsymbol{K}_1=\eta_2\begin{bmatrix} \bar{\eta}\tilde{k} & -\bar{\eta}\tilde{k} & 0 \\ -\bar{\eta}\tilde{k} & \bar{\eta}\tilde{k}+1 & -1 \\ 0 & -1 & 1 \end{bmatrix},\ \boldsymbol{K}=\begin{bmatrix} 2\bar{k}(1-coska)+\tilde{k} & -\tilde{k} & 0 \\ -\tilde{k} & \tilde{k}+1 & -1 \\ 0 & -1 & 1 \end{bmatrix} \quad (5)$$

where $m_1/m_4=\bar{m}$, $m_3/m_4=\tilde{m}$, $k_1/k_4=\bar{k}$, $k_3/k_4=\tilde{k}$.

Upon introducing the state vector$\boldsymbol{X}(t)=[q^T \quad \dot{q}^T]^T$, Eq. (4) is rewritten in state-space form as

$$\boldsymbol{X}(t)=\boldsymbol{A}_2\boldsymbol{X}(t) \quad (6)$$

where $\boldsymbol{A}_2=\begin{bmatrix} \boldsymbol{0} & \boldsymbol{I} \\ -\boldsymbol{M}^{-1}(\boldsymbol{iK_1}+\boldsymbol{K}) & \boldsymbol{0} \end{bmatrix}$.

So we can obtain the standard eigenvalue equation of MMM model with viscous damping or structural damping

$$|\lambda\boldsymbol{I}-\boldsymbol{A}_i|=0,\ \ i=1,2. \quad (7)$$

The characteristic equation is obtained

$$\lambda^6+a\lambda^5+b\lambda^4+c\lambda^3+d\lambda^2+e\lambda+f=0, \quad (8)$$

The root of Eq. (8) is calculated as

$$\lambda_s(k)=Re(\lambda_s)\pm iIm(\lambda_s),\ s=1,2,3, \quad (9)$$

where damping ratio $\xi_s=Re(\lambda_s)/Abs(\lambda_s)$, and s represents the branch number.

In this paper, the Young's modulus of viscoelastic material is complex, the viscoelastic membranes act as structural damping. Numerical example only for structural damping is provided, correspondingly.

2.2. MM model

For comparison, motion equations of MM model is yielded as follows

$$m_1\ddot{u}_1^n+k_1(2u_1^n-u_1^{n-1}+u_1^{n+1})+k_2(u_1^n-u_2^n)+c_0(\dot{u}_1^n-\dot{u}_2^n)=0, \quad (10a)$$

$$m_2\ddot{u}_2^n+c_0(\dot{u}_2^n-\dot{u}_1^n)+k_2(u_2^n-u_1^n)=0. \quad (10b)$$

For the case of viscous damping, dispersion relation of MM model has been analyzed [18]. We only consider relation with structural damping here.

When structural damping is considered, dissipation force $f=c\dot{u}=i\eta ku$, Eq. (10a) and (10b) can be rewritten as

$$m_1\ddot{u}_1^n + k_1(2u_1^n - u_1^{n-1} - u_1^{n+1}) + k_2(u_1^n - u_2^n) + i\eta(k_2u_1^n - k_2u_2^n) = 0, \tag{11a}$$

$$m_2\ddot{u}_2^n + i\eta(k_2u_2^n - k_2u_1^n) + k_2(u_2^n - u_1^n) = 0. \tag{11b}$$

Substituting Eq. (2) into Eq. (11a) and (11b), we have

$$\widehat{\boldsymbol{M}}\ddot{\boldsymbol{q}} + i\eta\widehat{\boldsymbol{K}}_1\boldsymbol{q} + \widehat{\boldsymbol{K}}\boldsymbol{q} = 0, \tag{12}$$

Where $\widehat{\boldsymbol{M}} = \begin{bmatrix} m_1 & 0 \\ 0 & m_2 \end{bmatrix}$, $\widehat{\boldsymbol{K}}_1 = \begin{bmatrix} i\eta k_2 & -i\eta k_2 \\ -i\eta k_2 & i\eta k_2 \end{bmatrix}$, $\widehat{\boldsymbol{K}} = \begin{bmatrix} 2k_1 + k_2 - k_1e^{ika} - k_1e^{-ika} & -k_2 \\ -k_2 & k_2 \end{bmatrix}$, $\boldsymbol{q} = \begin{bmatrix} q_1(t) \\ q_2(t) \end{bmatrix} = [q_1(t) \quad q_2(t)]^T$.

Let $m_1/m_2 = \hat{m}$, $k_1/k_2 = \hat{k}$, $k_2/m_2 = \omega_{lr2}^2$, coefficient matrices of Eq. (12) can be rewritten as

$$\widehat{\boldsymbol{M}} = \frac{1}{\omega_{lr2}^2}\begin{bmatrix} \hat{m} & 0 \\ 0 & 1 \end{bmatrix}, \widehat{\boldsymbol{K}}_1 = \begin{bmatrix} 1 & -1 \\ -1 & 1 \end{bmatrix}, \widehat{\boldsymbol{K}} = \begin{bmatrix} 2\bar{k} + 1 - \bar{k}e^{ika} - \bar{k}e^{-ika} & -1 \\ -1 & 1 \end{bmatrix}. \tag{13}$$

Upon introducing the state vector $\boldsymbol{X}(t) = [q^T \quad \dot{q}^T]^T$, Eq. (12) is rewritten in state-space form as

$$\dot{\boldsymbol{X}}(t) = \boldsymbol{A}_3\boldsymbol{X}(t), \tag{14}$$

where $\boldsymbol{A}_3 = \begin{bmatrix} \boldsymbol{0} & \boldsymbol{I} \\ -\widehat{\boldsymbol{M}}^{-1}(i\widehat{\boldsymbol{K}}_1 + \widehat{\boldsymbol{K}}) & \boldsymbol{0} \end{bmatrix}$.

So we can obtain the standard eigenvalue equation of MM model considering structural damping

$$|\lambda\boldsymbol{I} - \boldsymbol{A}_3| = 0. \tag{15}$$

The characteristic equation is obtained

$$\lambda^4 + a\lambda^3 + b\lambda^2 + c\lambda + d = 0. \tag{16}$$

The roots of Eq. (16) may be expressed as

$$\lambda_s(k) = Re(\lambda_s) \pm iIm(\lambda_s), s = 1,2. \tag{17}$$

For numerical simulations, some parameters are introduced for MM model and MMM model: $\bar{k} = \tilde{k} = \hat{k} = 1$, $k_1/k_4 = \bar{k}$, $k_3/k_4 = \tilde{k}$, $\omega_{lr1} = \omega_{lr2} = 100$, $\bar{m} = 19$, $\tilde{m} = 5$, $\hat{m} = 19/6$ ($m_2 = m_3 + m_4$). The influence of structural damping on frequency band structure and damping ratio band structure are analyzed.

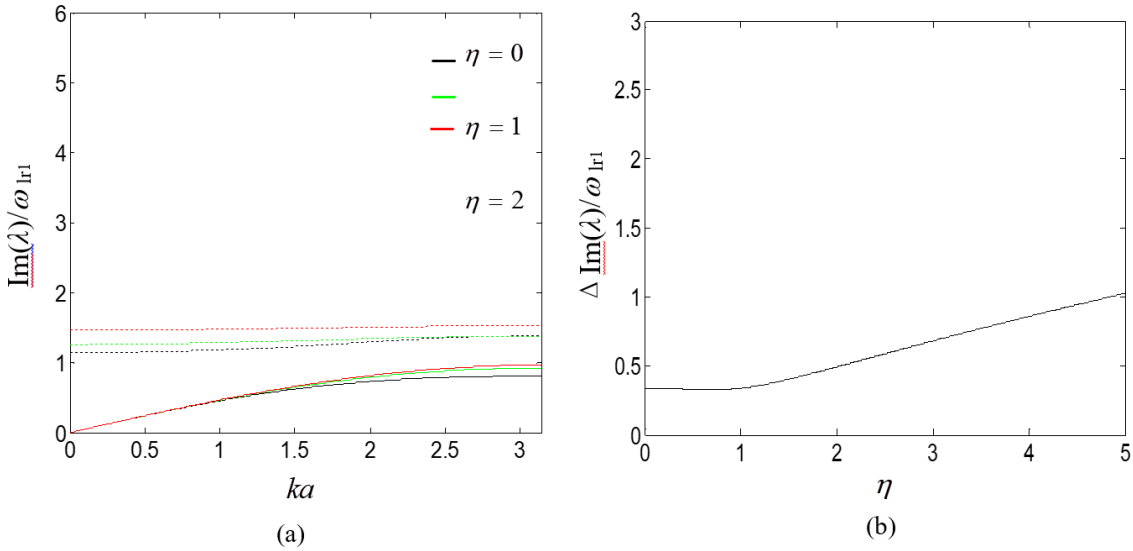

Figure 3(a). Frequency band structure and (b) band gap as a function of structural damping for the MM model

Fig. 3(a) displays the frequency band structure of the MM model with structural damping. Acoustic branches are represented by solid lines and optical branches by dot lines. Fig. 3(b) shows relations of the relative size of the band gap with structural damping, and it can be observed that although the value of structural damping is finite, the relative size of the band gap increases with the increase of structural damping. It is different from viscous damping. The results of damping ratio band structure for $\eta = 1$ and $\eta = 2$ are shown in Fig. 4. ξ_s means the sum of values for the acoustic and optical branches, i.e., $\xi_s = \xi_1 + \xi_2$ for the MM model. It is clear that damping ratio increase with increasing of the structural damping for the acoustic and optical branches from Fig. 4(a) and 4(b).

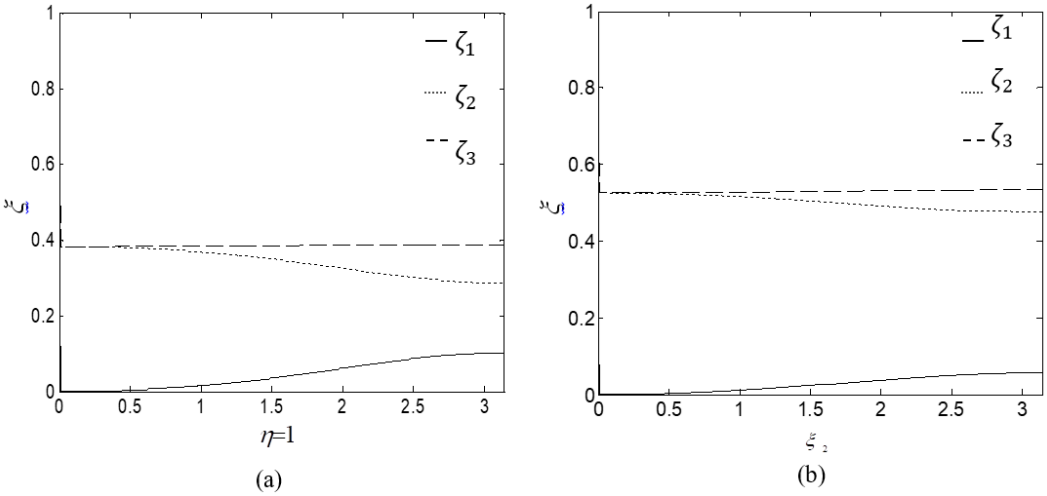

Figure 4. Damping ratio band structure corresponding to (a) $\eta = 1$ and (b) $\eta = 2$ for the MM model

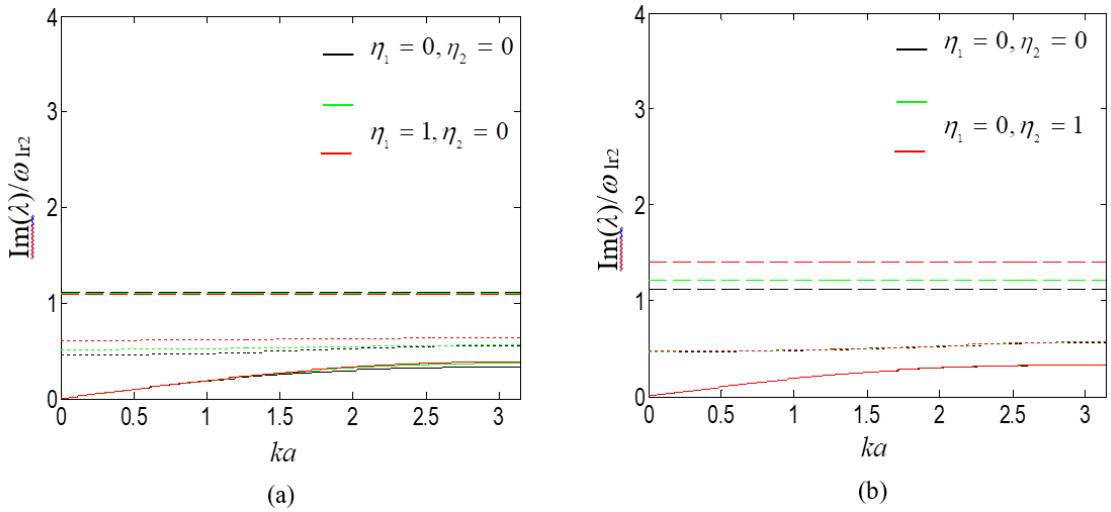

Figure 5. Frequency band structure considering the influence of structural damping (a) η_1 and (b) η_2 for the MMM model

In Fig. 5, Fig. 6 and Fig. 7, the first optical branch and second branch are represented by dash line and dot lines respectively, and acoustic branch is represented by the solid line. The influences of structural damping η_1 and η_2 on band structure and damping ratio are considered. It is observed that the second optical branch is more affected by η_1 than the second optical branch and acoustical branch from Fig. 5(a), and damping ratio of the second optical branch increases more rapidly than that of the first optical branch and acoustical branch from Fig. 6. As η_1 increases, the band gap will narrow between the first optical branch and the second optical branch, and the band gap will wide between the second optical branch and the acoustical branch. Fig. 5(b) shows the first optical branch is more affected by η_2 than the second optical branch and the acoustical branch. As η_2 increases, the band gap will wide between the first optical branch and the second optical branch.

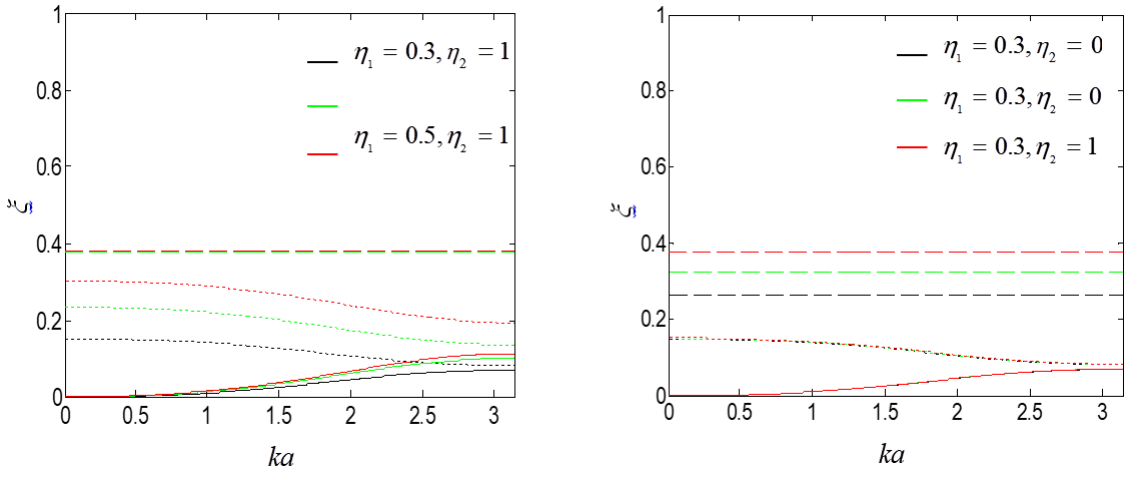

Figure 6. Damping ratio band structure for the MMM model

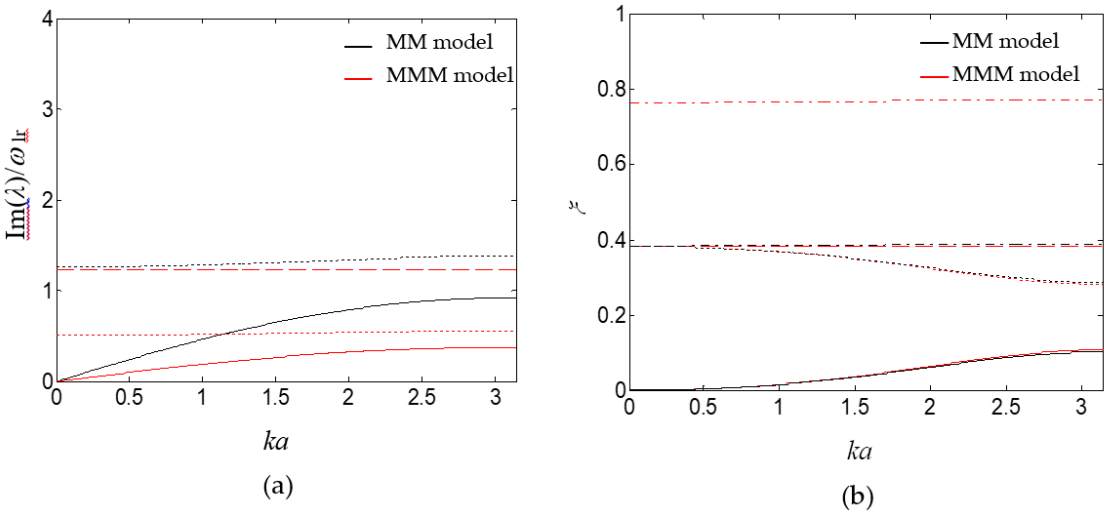

Figure 7(a). Frequency band structure and (b) damping ratio band structure for MM model and MMM model when $\eta = \eta_1 = \eta_2 = 1$

Fig. 7(a) shows the frequency band structure of two models. The results show that there are two band gaps in the MMM model, and band gap of MMM model might be bigger than that of MM model in width through adjusting η_1 and η_2. Fig. 7(b) displays the damping ratio band structure of two models. ξ_s means the sum of values for the acoustic and optical branches, i.e., $\xi_s = \xi_1 + \xi_2 + \xi_3$ for the MMM model. ξ_s is represented by the dash-dot line here. It can be concluded that MMM model exhibits higher damping ratio across the entire Brillouin zone for total damping ratio ξ_s. Next, the beam-type metamaterials based on MM model and MMM model are designed to prove the effectiveness of this conclusion.

3. Finite element model of the proposed beam-type acoustic metamaterial

The metamaterial beams are divided into four-node rectangular finite plate bending elements with 3 degrees of freedom per node as shown in Fig. 8. The beam based on the MM model is modeled with 567 four-noded rectangular elements with 640 nodes as shown in Fig. 8(a), the beam based on the MMM model is modeled with 630 four-noded rectangular elements with 704 nodes as shown in Fig. 8(b). The two models have the same length, width and thickness. The mass of local resonator in MM model is close to the sum of mass of local resonator and hollow mass in MMM model. The two models have the same lattice constant. For each node i, the degrees of freedom are the transverse displacement in the z -direction and the corresponding angular deflections in the x and y directions, as shown in Fig. 8(c). The finite element method based on Kirchhoff's plate theory from Ref [25] is adopted.

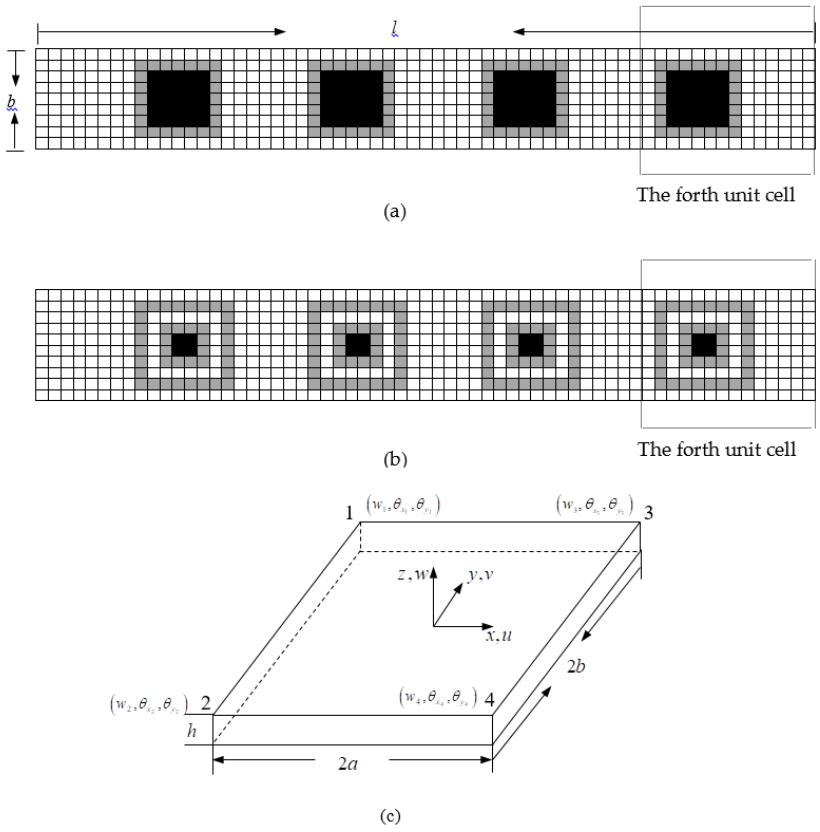

Figure 8. Finite element mesh of a four-node rectangular finite metamaterial beam (a) for MM model, (b) for MMM model and (c) a schematic diagram of a single element of the finite element model

It is necessary to point out that modulus for viscoelastic materials E is complex, which is expressed as

$$E = E' + E''i = E'(1 + \eta i), \tag{18}$$

where $E'$is storage modulus and η is known as the loss factor. Complex modulus embodies the elastic and dissipative properties of viscoelastic materials. Modulus for viscoelastic materials is dynamically identical to complex stiffness of spring in MM and MMM models. So the viscoelastic materials act as structural damping, not viscous damping.

4. Frequency response of the beam-type acoustic metamaterials

The computation of the frequency response is carried out on four different beams prototypes cantilevered from the left hand side, as shown in Fig. 9. A typical metamaterial beam consisting of periodic resonators surrounded by a rubber membrane embedded in aluminum matrix based on MM model is shown in Fig. 9(a). An aluminum beam has periodic cavities filled by a viscoelastic membrane that supports a hollow mass filled by a rubber membrane that supports a local resonator (as shown in Fig. 9(b)), an aluminum beam has periodic cavities filled

by a rubber membrane that supports a hollow mass filled by a viscoelastic membrane that supports a local resonator (as shown in Fig. 9(c)), and an aluminum beam with periodic cavities filled by a viscoelastic membrane that supports a hollow mass frame filled by a viscoelastic membrane that supports a local resonator (as shown in Fig. 9(d)) is designed based on MMM model. Four different beams prototypes are cantilevered from the left hand side ,which is 37.8cm in length, 5.4cm in width, and 0.15cm in thick. The material properties are listed in Table 1. Table 2 lists the first five natural frequencies of four different beams prototypes.

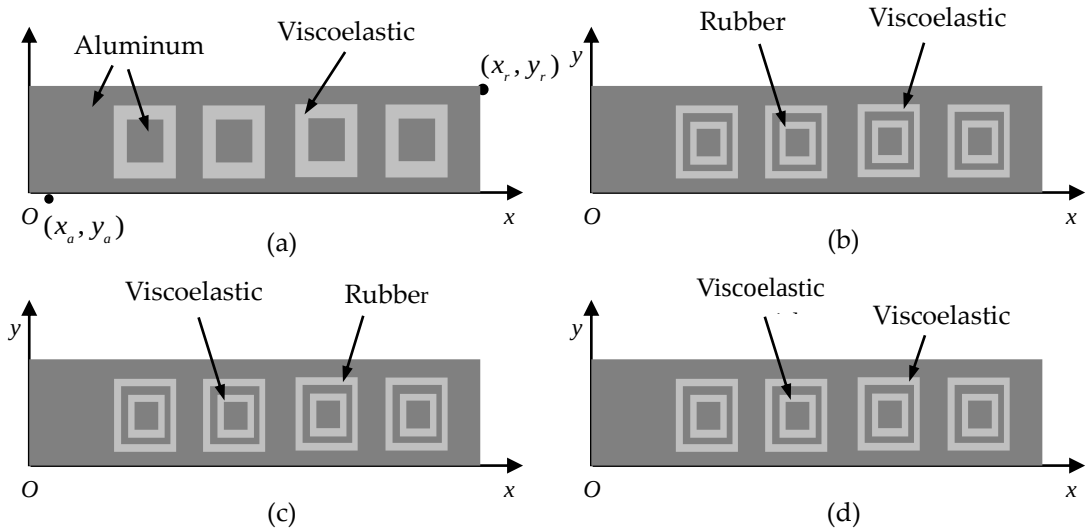

Figure 9. Structural models of the different configurations of beams. (a) beam 1, (b) beam 2, (c) beam 3, (d) beam 4

Table 1. Material properties

Materials	Yong's modulus E (Gpa)	poisson's ratio μ	Density ρ (kg/m^3)
Aluminum	70	0.30	2700
Rubber	0.195	0.50	1300
Polyurea	0.02(1+0.4i)	0.49	1018

Table 2. The first five natural frequencies of four different beams prototypes (Hz)

Prototypess	1st frequency	2nd frequency	3rd frequency	4th frequency	5th frequency
Beam 1	5.8	36.5	102.9	202.7	288.2
Beam 2	5.6	35.3	99.2	195.4	288.2
Beam 3	5.6	36.9	103.6	203.1	315.9
Beam 4	6.0	35.1	100.0	195.8	290.6

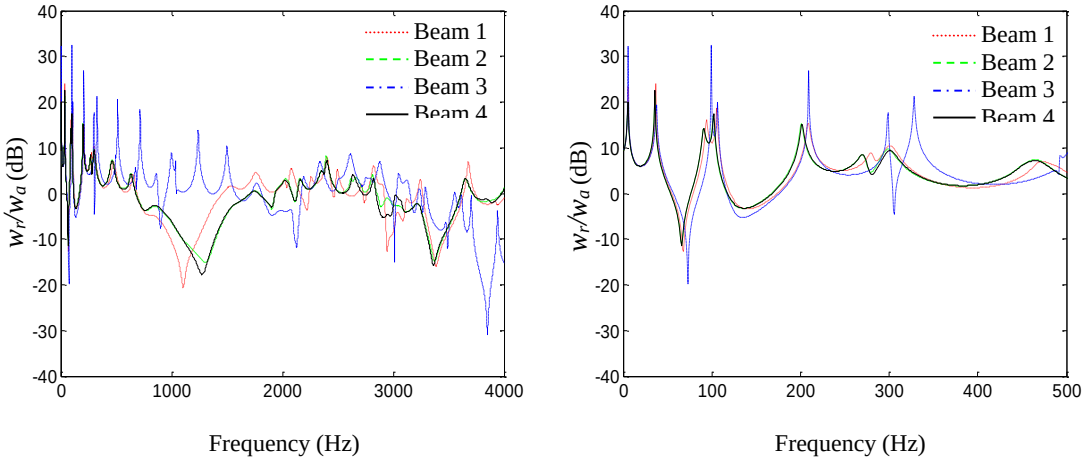

Figure 10. Frequency responses w_r over (a) 4000 Hz range and (b) 500 Hz range

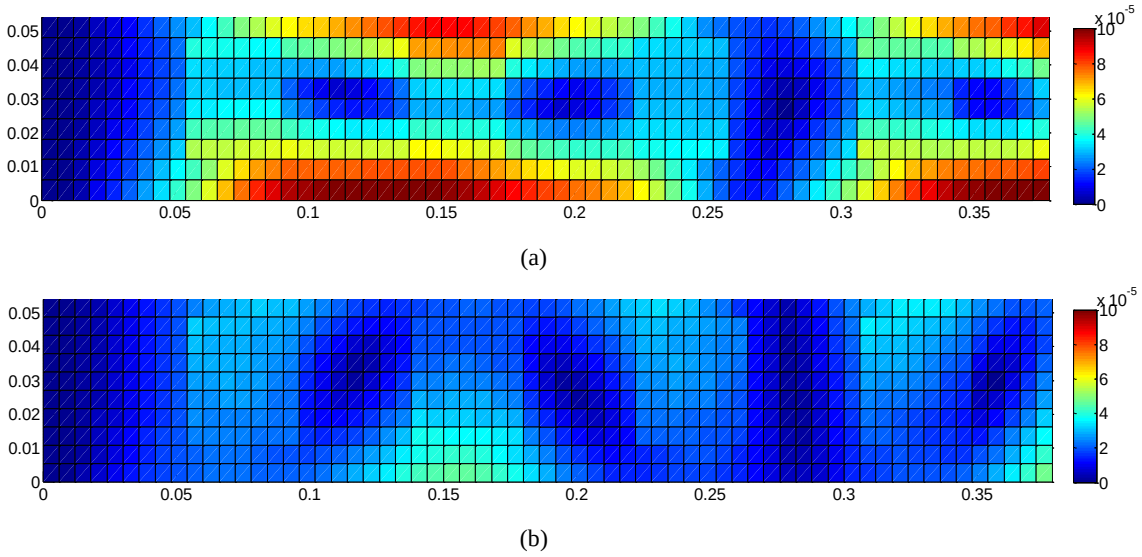

Figure 11. Frequency response under excitation frequencies at 280 Hz for (a) beam 1 and (b) beam 4

Fig. 10(a) and (b) display the magnitude of the transfer function w_r/w_abetween response w_r at point (x_r, y_r) and response w_a at point (x_a, y_a) for all beams (black stars in Fig. 9(a)).

$x_r = 0.378m$ and $y_r = 0.054m$. The excitation force with amplitude of 1N is applied at $x_a = 0.004m$ and$y_a = 0m$. The effectiveness of four beams in attenuating vibration is presented. Beam 2 and 4 clearly increases average vibration attenuation over the considered frequency range. Compared with beam 2, beam 4 shows clearly vibration attenuation at some frequency range, such as between 1178 Hz and 1280 Hz, between 2800 Hz and 3000 Hz. Beam 3 shows some attenuation at higher frequencies. It can be seen from Fig. 7 and 10 that The proposed metamaterial beam 4 based on the MMM model has the best vibration attenuation characteristics over the considered frequency range, and exhibits higher damping ratio across the considered frequency range.

Compared with beam 1 based on the MM model, it can be observed that beam 4 shows distinct stop bands along the considered frequency range, such as frequency range from 272 Hz to 280 Hz, from 1178 Hz to 1280 Hz. Vibration attenuation of beam 4 is also achieved particularly at low frequencies. w_r/w_aat the second bending mode for beam 1 is 24dB, w_r/w_aat the same mode for beam 4 is 22.5 dB. So vibration attenuation is increased by 6%. It can be calculated that the attenuation of the third bending mode is increased by 8%, and the attenuation of the fifth bending mode is increased by 10%. Fig. 11(a) and (b) show frequency response of beam 1 and 4 under excitation frequencies at 280 Hz. The force excitation position is same as Fig. 10. Significant vibration attenuation is observed for beam 4 because the excitation frequency falls into the distinct stop band.

Conclusions

A one-dimensional mass-in-mass-in-mass (MMM) model with structural damping is given, and then a typical mass-in-mass (MM) model with structural damping is also given for comparison. The MMM model exhibits higher damping and dissipation, resulting in elastic wave attenuation. A beam-type acoustic metamaterial with periodic cavities filled by a viscoelastic membrane that supports a hollow mass still filled by a viscoelastic membrane that supports a local resonator is designed based on MMM model with structural damping.

Flexural vibration of the designed beam-type acoustic metamaterial is studied theoretically as well as numerically. Another kind of beam-type acoustic metamaterial of same size and weight based on MM model with structural damping is presented for comparing to the designed metamaterial. It is found that the designed metamaterial is more effective in suppressing structural vibration. The base structure represents about 73% of the metamaterial structure's area and about 93% of the beam's weight is aluminum. In comparison to typical acoustic metamaterial of same size and weight, designed metamaterial structure has higher dissipation during the whole frequency range.

Acknowledgements

Supported by the National Natural Science Foundation of China under Grant number 11102047, and Science Foundation of Heilongjiang Province of China under Grant number. LC2016001.

References

An, X. Y., Fan, H. L., & Zhang, C. Z. (2020). Elastic wave and vibration bandgaps in planar square m- etamaterial-based lattice structures. *Journal of sound and vibration*, (475), 115292. https://doi.org/10.1016/j.jsv.2020.115292

Benchabane, S., Khelif, A., Robert, L., Rauch, J. Y., Pastureaud, T., & Laude, V. (2006). Elastic band gaps for surface modes in an ultrasonic lithium niobate phononic crystal. *Photonic crystal materials and devices*, (6182), 618216. https://doi.org/10.1117/12.662220

Cenedese, M., Belloni, E., & Braghin, F. (2021). Interaction of Bragg scattering bandgaps and local resonators in mono-coupled periodic structures. *Journal of applied physics*, 129(12), 124501. https://doi.org/10.1063/5.0038438

Chen, Y. Y., Barnhart, M. V., Chen, J. K., Hu, G. K., Sun, C. T., & Huang, G. L. (2016). Dissipative elastic metamaterials for broadband wave mitigation at subwavelength scale. Composite Structures, 136, 358-371. https://doi.org/10.1016/j.compstruct.2015.09.048

Cinefra, M., de Miduel, A. G., Filippi, M., Houriet, C., Pagni, A., & Carrera, E. (2021). Homogenization and free-vibration analysis of elastic metamaterial plates by Carrera unified Formulation finite elements . *Mechanics of Advanced Materials and Structures*, 28(5), 476-485. https://doi.org/10.1080/15376494.2019.1578005

Ding, Y., Liu, Z., Qiu, C., & Shi, J. (2007). Metamaterial with simultaneously negative bulk mod- ulus and mass density. *Physical review letters*, 99 (9), 093904. https://doi.org/10.1103/PhysRevLett.99.093904

Fok, L., Ambati, M., & Zhang, X. (2008). Acoustic metamaterials. *MRS Bulleyin*, 33(10)931-934. https://doi.org/10.1557/mrs2008.202

Galich, P. I., Fang, N. X., Boyce, M. C., & Rudykh, S. (2017). Elastic wave propagation in finitely deformed layered materials. Journal of the Mechanics and Physics of Solids, 98, 390-410. https://doi.org/10.1016/j.jmps.2016.10.002

Gao, P. L., Climenta, A., Sanchez-Dehesa, J., & Wu, L. Z. (2019). Single-phase metamaterial plates for broadband vibration suppression at low frequencies. *Journal of sound and vibration*, 444, 108-126. https://doi.org/10.1016/j.jsv.2018.12.022

Huang, G. L., & Sun, C. T. (2010). Band gaps in a multiresonator acoustic metamaterial. Journal of vibration and acoustics-transactions of the ASME, 132(3) 031003. https://doi.org/10.1115/1.4000784

Hussein, M. I., & Frazier, M. J. (2013). Metadamping in dissipative metamaterials. Proceedings of the ASME 2013 IMECE, San Diego, California, USA, V014T15A051.

Hussein, M. I., & Frazier, M. J. (2013). Metadamping: an emergent phenomenon in dissipative metamaterials. *Journal of sound and vibration*, 332 (20), 4767-4774. https://doi.org/10.1016/j.jsv.2013.04.041

Hussein, M. I., Leamy, M. J., & Ruzzene, M. (2014). Dynamics of phononic materials and structures: Historical origins, recent progress, and future outlook. *Applied Mechanics Reviews*, 66(4). https://doi.org/10.1115/1.4026911

Li, J. Q., Fan, X. L., & Li, F. M. (2020). Numerical and experimental study of a sandwich-like metama-terial plate for vibration suppression. *Composite structures*, (238), 111969. https://doi.org/10.1016/j.compstruct.2020.111969

Li, S. B., Dou, Y. H., Chen,T. N., Wang, Z. G., & Guan, Z. R. (2018). A novel metal-matrix phononic crys-tal with a low-frequency, broad and complete, locally-resonant band gap. *Modern physics letters B*, 32(19), 1850221. https://doi.org/10.1142/S0217984918502214

Li, Y. G., Zhu, L., & Chen. T. N. (2017). Plate-type elastic metamaterials for low frequency broad-band elastic wave attenuation. *Ultrasonics*, 73, 34-42. https://doi.org/10.1016/j.ultras.2016.08.019

Liu, Z. Y., Zhang, X. X., Mao, Y. W., Zhu, Y. Y., Yang, Z. Y., Chan, C. T., & Sheng, P. (2000). Locally resonant sonic materials. *Science*, 289 (5485) 1734-1736. https://doi.org/10.1126/science.289.5485.1734

Muhammad, & Lim, C. W. (2019). Elastic waves propagation in thin plate metamaterials and evidence of low frequency pseudo and local resonance bandgaps. *Physics Letters A*, 383(23), 2789-2796. https://doi.org/10.1016/j.physleta.2019.05.039

Nouh, M. A., Aldraihem, O. J., & Baz, A. (2016). Periodic metamaterial plates with smart tunable local resonators. *Journal of Intelligent Material Systems and Structures*, 27(13), 1829-1845. https://doi.org/10.1177/1045389x15615965

Nouh, M., Aldraihem, O. & Baz, M. (2014). Vibration Characteristics of Metamaterial Beams with periodic Local Resonances. *Journal of vibration and acoustics-transactions of the ASME*, 136(6), 061012. https://doi.org/10.1115/1.4028453

Pai, P. F. (2010). Metamaterial-based broadband elastic wave absorber. *Journal of intelligent material systems and structures*, 21(5), 517-528. https://doi.org/10.1177/1045389X09359436

Pai, P. F. (2014). Acoustic metamaterial beams based on multi-frequency vibration absorbers. *International journal of mechanical sciences*, 79, 195-205. https://doi.org/10.1016/j.ijmecsci.2013.12.013

Peng, H., Pai, P. F., & Deng, H. G. (2015). Acoustic multi-stopband metamaterial plates design for broadband elastic wave absorption and vibration suppression. *International journal of mechanical sciences*, 103, 104-114. https://doi.org/10.1016/j.ijmecsci.2015.08.024

Raghavan, L., & Phani, A. (2013). Local resonance bandgaps in periodic media: theory and experiment. *Journal of the acoustical society of America*, 134 (3), 1950-1959. https://doi.org/10.1121/1.4817894

Sun, H., Du, X., & Pai, P. F. (2010). Theory of metamaterial beams for broadband vibration abso-rption. *Journal of intelligent material systems and structures*, 21(11), 1085-1101. https://doi.org/10.1177/1045389X10375637

Suobin, Li., Dou, Y. H., Chen, T. N., Xu, J. N., Li, B., & Zhang, F. (2019). Designing a broad locally-resonant bandgap in a phononic crystals. *Physics Letters A*, 383(12), 1371-1377. https://doi.org/10.1016/j.physleta.2019.01.061

Wang, T., Sheng, M. P., Guo, Z. W., & Qin, Q. H. (2016). Flexural wave suppression by an acoustic metamaterial plate. *Applied acoustics*, 114, 118-124. https://doi.org/10.1016/j.apacoust.2016.07.023

Zhong, H. B., Tian, Y. J., Gao, N. S., Lu, K., & Wu. J. H. (2021). Ultra-thin composite underwater hon-eycomb-type acoustic metamaterial with broadband sound insulation and high hydro-static pressure resistance. *Composite structures*, (227), 114603. https://doi.org/10.1016/j.compstruct.2021.114603

Zhou, W.J., Wu, B., Su, Y. P., Liu, D. Y., Chen, W. Q., & Bao, R. H. (2021). Tunable flexural wave band gaps in a prestressed elastic beam with periodic smart resonators. *Mechanics of advanced materials and structures*, 28(3), 221-228. https://doi.org/10.1080/15376494.2018.1553261

Zhu, R., Huang, G. L., Huang, H. H., & Sun, C. T. (2011). Experimental and numerical study of guided wave propagation in a thin metamaterial plate. *Physics letters A*, 375, 2863-2867. https://doi.org/10.1016/j.physleta.2011.06.006